



# Tau pathology as determinant of changes in atrophy and cerebral blood flow: a multi-modal longitudinal imaging study

Denise Visser<sup>1,2,3</sup> · Sander C. J. Verfaillie<sup>1,2,3,4</sup> · Iris Bosch<sup>1,3,5,6</sup> · Iman Brouwer<sup>1,2,3</sup> · Hayel Tuncel<sup>1,2,3</sup> · Emma M. Coomans<sup>1,2,3</sup> · Roos M. Rikken<sup>1,2,3</sup> · Sophie E. Mastenbroek<sup>1,2,3,7</sup> · Sandeep S. V. Golla<sup>1,2,3</sup> · Frederik Barkhof<sup>1,2,3,8</sup> · Elsmarieke van de Giessen<sup>1,2,3</sup> · Bart N. M. van Berckel<sup>1,2,3</sup> · Wiesje M. van der Flier<sup>2,9,10</sup> · Rik Ossenkoppele<sup>2,7,9</sup>

Received: 20 January 2023 / Accepted: 13 March 2023  
© The Author(s) 2023

## Abstract

**Purpose** Tau pathology is associated with concurrent atrophy and decreased cerebral blood flow (CBF) in Alzheimer's disease (AD), but less is known about their temporal relationships. Our aim was therefore to investigate the association of concurrent and longitudinal tau PET with longitudinal changes in atrophy and relative CBF.

**Methods** We included 61 individuals from the Amsterdam Dementia Cohort (mean age  $65.1 \pm 7.5$  years, 44% female, 57% amyloid- $\beta$  positive [ $A\beta+$ ], 26 cognitively impaired [CI]) who underwent dynamic [ $^{18}\text{F}$ ]flortaucipir PET and structural MRI at baseline and  $25 \pm 5$  months follow-up. In addition, we included 86 individuals (68 CI) who only underwent baseline dynamic [ $^{18}\text{F}$ ]flortaucipir PET and MRI scans to increase power in our statistical models. We obtained [ $^{18}\text{F}$ ]flortaucipir PET binding potential ( $BP_{\text{ND}}$ ) and  $R_1$  values reflecting tau load and relative CBF, respectively, and computed cortical thickness from the structural MRI scans using FreeSurfer. We assessed the regional associations between i) baseline and ii) annual change in tau PET  $BP_{\text{ND}}$  in Braak I, III/IV, and V/VI regions and cortical thickness or  $R_1$  in cortical gray matter regions (spanning the whole brain) over time using linear mixed models with random intercepts adjusted for age, sex, time between baseline and follow-up assessments, and baseline  $BP_{\text{ND}}$  in case of analyses with annual change as determinant. All analyses were performed in  $A\beta-$  cognitively normal (CN) individuals and  $A\beta+$  (CN and CI) individuals separately.

**Results** In  $A\beta+$  individuals, greater baseline Braak III/IV and V/VI tau PET binding was associated with faster cortical thinning in primarily frontotemporal regions. Annual changes in tau PET were not associated with cortical thinning over time in either  $A\beta+$  or  $A\beta-$  individuals. Baseline tau PET was not associated with longitudinal changes in relative CBF, but increases in Braak III/IV tau PET over time were associated with increases in parietal relative CBF over time in  $A\beta+$  individuals.

**Conclusion** We showed that higher tau load was related to accelerated cortical thinning, but not to decreases in relative CBF. Moreover, tau PET load at baseline was a stronger predictor of cortical thinning than change of tau PET signal.

**Keywords** Tau PET · Cerebral blood flow · Atrophy · Alzheimer's disease · Longitudinal

## Introduction

Histopathological and in vitro studies have shown that tau pathology is closely associated with neuronal injury (synaptic alterations and neuronal loss) in Alzheimer's disease (AD) [1–6]. The positron emission tomography (PET) tracer [ $^{18}\text{F}$ ]

flortaucipir binds to paired helical filaments of tau and has enabled examination of the relationship between tau pathology and neuronal injury or neurodegeneration in vivo in AD [7–10]. In line with histopathological and in vitro studies, neuroimaging studies have demonstrated strong correlations between baseline tau PET with cross-sectional atrophy in AD patients ([1, 10, 11]). In addition, longitudinal studies with relatively short follow-up time (i.e., 12–15 months) have shown that tau load also predicts future atrophy rates [2, 5, 11–13]. To better understand how tau PET and neurodegeneration are related, it is important to study their dynamic associations over time and investigate how baseline tau load and change in tau load associate with longitudinal cortical thinning.

This article is part of the Topical Collection on Neurology – Dementia

✉ Denise Visser  
d.visser2@amsterdamumc.nl

✉ Rik Ossenkoppele  
r.ossenkoppele@amsterdamumc.nl

Extended author information available on the last page of the article

Another aspect of neuronal injury in AD is the progressive reduction of cerebral blood flow (CBF). Dynamic scanning protocols can be utilized to obtain a measure of  $R_1$  [14, 15].  $R_1$  is a proxy for relative cerebral blood flow (rCBF) and is closely associated with metabolic activity ( $[^{18}\text{F}]\text{FDG}$  PET) and  $^{15}\text{O}\text{-H}_2\text{O}$  PET (i.e., the “gold standard” for measuring flow) [16–18]. Previous studies using other imaging techniques such as arterial spin labeling (ASL) to measure CBF have demonstrated decreased CBF (or cerebral perfusion) in (probable) AD patients [19, 20]. When it comes to the relationship between tau pathology and CBF (cross-sectional), it has been shown that higher levels of tau pathology are associated with locally decreased rCBF in AD [14, 21]. Taken together, these studies indicate that baseline tau pathology is related to neuronal injury as reflected by decreased CBF as well as atrophy in AD. However, it is less well established whether (rate of) change in tau pathology also relates to (rate of) change in CBF.

With respect to the order of pathophysiological processes in AD, general consensus has been reached for accumulation of tau pathology (relatively early event) and atrophy (relatively late event) [4, 22]. There is less agreement regarding rCBF changes, as some studies suggest CBF to be an early biomarker of disease [19], while others suggest changes in CBF to potentially be both cause and consequence of protein accumulation [23]. Many studies suggested that neuronal injury imaging markers change relatively late in the disease process, after the first observation of protein accumulation (such as amyloid or tau pathology) on PET or in CSF [4, 21, 22, 24]. The aim of this longitudinal study was to investigate the associations between changes in tau PET with imaging biomarkers of neuronal injury (i.e., atrophy and CBF) in a cohort comprising i) amyloid negative ( $\text{A}\beta^-$ ) cognitively normal (CN) individuals, and ii) amyloid positive ( $\text{A}\beta^+$ ) CN and cognitively impaired (CI) (AD-phenotype) individuals. First, we assessed whether tau PET, atrophy, and rCBF showed significant changes over time. Second, we assessed the association between (i) baseline and (ii) annual change in tau PET (binding potential  $[\text{BP}_{\text{ND}}]$ ) and longitudinal changes in both cortical thickness and rCBF ( $R_1$ ). Assuming that CBF alterations occur in between tau accumulation and atrophy in the pathophysiological development of AD, we hypothesized that higher tau load at baseline would be strongly associated with a steeper decline in cortical thickness and rCBF in  $\text{A}\beta^+$  individuals. Furthermore, we hypothesized that larger increases in tau PET over time would be associated with larger decreases in cortical thickness and rCBF in  $\text{A}\beta^+$  individuals.

## Methods

### Participants

We included 61 individuals from the Amsterdam Dementia Cohort (ADC) of the Alzheimer Center Amsterdam [25] of whom 26 were CN  $\text{A}\beta^-$  with subjective cognitive decline (SCD) [26] and 35  $\text{A}\beta^+$  with SCD (CN,  $n=9$ ), or cognitively impaired AD (CI,  $n=26$ ) [27, 28]. All 61 participants underwent baseline and 2-year follow-up dynamic  $[^{18}\text{F}]\text{florbetapir}$  PET and MRI scans, and are referred to as the follow-up sample. In addition, to increase power in our statistical models, we included 86 individuals from the ADC (18 CN and 68 CI) who only underwent baseline dynamic  $[^{18}\text{F}]\text{florbetapir}$  PET and MRI scans, referred to as the baseline-only sample. Individuals with SCD ( $n_{\text{follow-up} + \text{baseline-only}} = 55$ ) were recruited from the SCIENCE cohort [29], which is part of the ADC [25]. All individuals underwent a standardized diagnostic workup, including medical and neurological examination, assessment of vital functions, informant-based history, neuropsychological evaluation, magnetic resonance imaging (MRI), and standard labs. Subsequently, diagnoses were determined by consensus in a multidisciplinary meeting. AD biomarkers in cerebrospinal fluid (CSF) and/or  $\text{A}\beta$  PET were available for all individuals. Individuals were classified as  $\text{A}\beta^+$  based on abnormal AD biomarkers (CSF  $\text{A}\beta_{42} < 813$  pg/mL [30] and/or abnormal  $\text{A}\beta$  PET (on visual read)). When both CSF  $\text{A}\beta_{42}$  and  $\text{A}\beta$  PET were available,  $\text{A}\beta$  PET was used for the determination of  $\text{A}\beta$  status. All AD patients had abnormal AD biomarkers and are therefore considered in the AD pathophysiological continuum, according to the NIA-AA Research Framework, classified as  $\text{A}\beta^+$  CI individuals [22]. Individuals with SCD with evidence of  $\text{A}\beta$  pathology were classified as  $\text{A}\beta^+$  CN individuals. Amyloid- $\beta$  status was only determined at baseline. Exclusion criteria included severe traumatic brain injury, abnormalities on MRI likely to interfere with segmentation of tau PET and participation in a drug trial with tau or  $\text{A}\beta$ -targeting agents. Individuals were grouped based on amyloid status (negative and positive) for analyses. The study is in accordance with the ethical standards of the Medical Ethics Review Committee of the Amsterdam UMC VU Medical Center and with the 1964 Helsinki Declaration and its later amendments. Written informed consent was obtained from all participants prior to participation.

### Image acquisition

All 61 individuals from the follow-up sample underwent dynamic  $[^{18}\text{F}]\text{florbetapir}$  PET and MRI scans at baseline and 2-year follow-up. Dynamic  $[^{18}\text{F}]\text{florbetapir}$  PET scans

were acquired on a PET-CT scanner (Philips Medical Systems, Best, The Netherlands) at the Amsterdam UMC VU Medical Center. Individual doses of [ $^{18}\text{F}$ ]flortaucipir were synthesized on site, using a previously described protocol [31]. All individuals at baseline participated in an initial scanning protocol of 130 min, consisting of a 60-min dynamic emission scan, a 20-min break, and another dynamic emission scan between 80 and 130 min post-injection [31]. In order to lower the burden associated with a long scanning protocol, especially for AD patients, our research group recently validated a quantitatively accurate shortened scanning protocol of 100 min [32]. Subsequently, all CI AD patients participating in follow-up PET scans for our ongoing longitudinal cohort study participated in the recently validated scanning protocol of 100 min, consisting of a 30-min dynamic emission scan, a 50-min break, and a second dynamic emission scan between 80 and 100 min post-injection. In order to correct for this adjusted scanning protocol at follow-up, the 130-min baseline scans of these individuals were analyzed as biphasic 100-min scans ( $n=26$ ). Scanning protocols were initiated with a low-dose CT for attenuation correction, followed by simultaneously injecting  $\sim 240 \pm 10$  MBq [ $^{18}\text{F}$ ]flortaucipir (bolus) and starting the first dynamic emission scan. After a break and a second low-dose CT for attenuation correction, another dynamic emission scan was performed. During scan procedures, head movements were restricted by a headband and head positioning was regularly checked using laser beams. PET scans were reconstructed with a matrix size of  $128 \times 128 \times 90$  and a voxel size of  $2 \times 2 \times 2$  mm<sup>3</sup>, including standard corrections for attenuation, dead time, randoms, decay, and scatter. For each scan protocol, the later dynamic PET scan was coregistered to the first dynamic PET scan into a single dataset. Furthermore, all individuals underwent a structural whole-brain MRI scan on a 3.0 Tesla (3 T) MRI scanner at baseline and follow-up (Ingenuity Time-of-Flight (Phillips medical systems, Best, The Netherlands)). The scanning protocol for the Ingenuity Time-of-Flight scanner included an isotropic structural 3D T1-weighted image using a sagittal turbo gradient-echo sequence (1.00 m<sup>3</sup> isotropic voxels, repetition time = 7.9 ms, echo times = 4.5 ms and flip angle = 8°) and a 3D fluid-attenuated inversion recovery (FLAIR) image (1.04 × 1.04 × 1.12 mm voxels, repetition time = 4800 ms, echo time = 278.8 ms, flip angle 90°). The 86 individuals from the baseline-only sample only underwent the above-described dynamic [ $^{18}\text{F}$ ]flortaucipir PET and MRI scans at baseline.

### PET image analysis

PET image analysis has been described previously [14, 31, 32]. Briefly, individual T1-weighted MRI scans were co-registered to native PET space, using Vinci software

(Max Plank Institute, Cologne, Germany). The Hammers and Svarer templates incorporated in PVElab software were used to define cortical gray matter regions of interest (ROIs) on the co-registered MRI scans [33, 34]. Receptor parametric mapping (RPM) was applied to the PET data to obtain parametric images of  $\text{BP}_{\text{ND}}$  and  $R_1$ , with the cerebellum gray matter as a reference region [35]. Previous research from our group has demonstrated that RPM is the best parametric method for [ $^{18}\text{F}$ ]flortaucipir [36], and has an excellent test-retest repeatability [9]. Tau PET data were additionally partial volume corrected using Van Cittert iterative deconvolution methods (IDM), combined with highly constrained back-projections (HYPR) as described previously [14]. Since results remained essentially unchanged when using partial-volume corrected (PVC) data, only non-partial volume corrected data are presented throughout the manuscript. We obtained  $\text{BP}_{\text{ND}}$  values (bilateral volume-weighted average) in three a priori defined regions corresponding to Braak staging regions of tau pathology (Braak I, Braak III/IV, and Braak V/VI), as described previously [10]. For  $R_1$  we used all cortical gray matter ROIs as available in the Hammers template, with addition of the entorhinal ROI from the Svarer template.

### MR image analysis

Cortical thickness (in mm) was obtained using FreeSurfer version 6.0.1 (<https://surfer.nmr.mgh.harvard.edu/>). MR images from individuals with longitudinal data were processed through the recon-all longitudinal processing stream, including motion correction, skull-stripping, registration, segmentation, smoothing, and parcellation mapping [37]. Images from individuals who only underwent baseline scans were processed through the recon-all processing stream for single timepoints. For both processing streams, cortical parcellation was performed based on the Desikan-Killiany Atlas (DKT), which contains 34 regions per hemisphere [38]. In order to improve cortical segmentation, a combination of T1-weighted+FLAIR images was used as input [39]. For individuals with missing FLAIR data at baseline and/or follow-up, only T1-weighted images were used for cortical segmentation at all available time points ( $n_{\text{A}\beta^-} = 1$ ,  $n_{\text{A}\beta^+} = 3$  out of follow-up sample ( $n_{\text{total}} = 61$ );  $n_{\text{A}\beta^+} = 5$  out of baseline-only sample ( $n_{\text{total}} = 86$ )). Following all processing streams, segmentation, and parcellation qualities were manually inspected for gross abnormalities. For cortical thickness, we used all cortical gray matter ROIs as available in the DKT atlas.

### Statistical analysis

All analyses were performed for  $\text{A}\beta^+$  and  $\text{A}\beta^-$  individuals separately. To establish whether imaging markers changed

over time, we performed linear mixed effects models (LMMs) with global  $BP_{ND}$ ,  $R_1$ , or cortical thickness as dependent variable and time as determinant, adjusted for age-at-PET and sex (using both the follow-up and baseline-only sample). To assess differences in demographic variables and  $BP_{ND}$ ,  $R_1$ , and cortical thickness, between  $A\beta^-$  and  $A\beta^+$  individuals, two-sample  $t$ -tests were used. Associations between baseline  $BP_{ND}$  in our three regions of interest (Braak I, Braak III/IV, and Braak V/VI) and cortical thickness or  $R_1$  over time (in all cortical regions available in the brain templates) were assessed using LMMs with random intercepts and fixed slopes, adjusted for age, sex and time between baseline and follow-up assessments. For these analyses individuals from both the follow-up and baseline-only samples were used ( $n_{total} = 147$ ). Next, the associations between annual change in  $BP_{ND}$  and longitudinal cortical thickness or  $R_1$  were assessed using the same LMMs, now with annual change in  $BP_{ND}$  as predictor and additionally adjusted for baseline  $BP_{ND}$ . Therefore, annual change for  $BP_{ND}$  was calculated for all three regions of interest (Braak I, III/IV, and V/VI) by subtracting the baseline value from the follow-up value and dividing by the time between measurements in years. For these analyses, only individuals from the follow-up sample were used ( $n = 61$ ). Results are reported both with and without the Benjamini-Hochberg False Discovery Rate (FDR) correction with a  $Q$  value of 5%. All statistical analyses were performed in Rstudio v4.0.3 and results are visualized using forest plots of the effect sizes and their respective confidence intervals. The regional associations are displayed using the ggseg R package for FDR-surviving cortical thickness ROIs only (since ggseg does not yet support the atlases used for  $R_1$ ).

## Results

### Participants

Out of the 61 individuals who underwent follow-up, 35 were  $A\beta^+$  and 26  $A\beta^-$  at baseline (Table 1, Fig. 1). Baseline demographics and characteristics of the total baseline sample (including the baseline-only sample,  $n = 147$ ) are shown in sTable 1. Relative to the total baseline sample, the follow-up sample consisted of younger patients, with relatively higher MMSE scores and higher levels of global tau PET  $BP_{ND}$ . In the follow-up sample,  $A\beta^+$  individuals were more often cognitively impaired (74% in  $A\beta^+$  vs 0% in  $A\beta^-$ ;  $p < 0.001$ ) and had lower MMSE scores when compared to  $A\beta^-$  individuals ( $26 \pm 3$  in  $A\beta^+$  vs  $29 \pm 1$  in  $A\beta^-$ ;  $p < 0.001$ ). Of the 61 individuals with longitudinal data,  $A\beta^+$  individuals had higher  $BP_{ND}$  values at both baseline and follow-up, whereas cortical thickness and  $R_1$  were lower (Table 1). Age, sex, and time between scans did not differ between  $A\beta^+$  and  $A\beta^-$  individuals.

### Longitudinal change

Tau PET  $BP_{ND}$  significantly increased over time in both  $A\beta^-$  and  $A\beta^+$  individuals, with the largest increases observed in the  $A\beta^+$  individuals (Table 1, Fig. 2). Cortical thickness decreased over time in  $A\beta^+$  individuals only. rCBF, however, did not significantly change over time in either  $A\beta^+$  or  $A\beta^-$  individuals (Table 1, Fig. 2). Although LMM results did not show a significant (average) change in rCBF on the group level, we did observe substantial changes at the individual level (both increases and decreases, potentially

**Table 1** Characteristics of the follow-up sample

|   | Total follow-up sample | Amyloid positive     | Amyloid negative  |
|---|------------------------|----------------------|-------------------|
| Sample, $n$                             | 61                     | 35                   | 26                |
| Age, years                              | $65.4 \pm 7.4$         | $66.3 \pm 7.2$       | $63.7 \pm 7.7$    |
| Female, $n$                             | 27                     | 15                   | 12                |
| Cognitively impaired, $n$               | 26                     | 26***                | 0                 |
| MMSE (baseline)                         | $27 \pm 3$             | $26*** \pm 3$        | $29 \pm 1$        |
| Time between MRI scans, minutes         | $25.9 \pm 7.2$         | $26.3 \pm 5.0$       | $25.3 \pm 9.2$    |
| Time between PET scans, minutes         | $25.2 \pm 3.7$         | $25.8 \pm 3.4$       | $24.5 \pm 4.0$    |
| Baseline global tau PET $BP_{ND}$       | $0.13 \pm 0.18$        | $0.22*** \pm 0.19$   | $0.02 \pm 0.03$   |
| Follow-up global tau PET $BP_{ND}$      | $0.19^b \pm 0.22$      | $0.30***^b \pm 0.23$ | $0.04^b \pm 0.03$ |
| Annual change global tau PET $BP_{ND}$  | $0.02 \pm 0.03$        | $0.04*** \pm 0.03$   | $0.01 \pm 0.01$   |
| Baseline global cortical thickness, mm  | $2.11 \pm 0.07$        | $2.08** \pm 0.07$    | $2.14 \pm 0.07$   |
| Follow-up global cortical thickness, mm | $2.09^a \pm 0.09$      | $2.05***^b \pm 0.08$ | $2.14 \pm 0.07$   |
| Annual change global cortical thickness | $-0.01 \pm 0.02$       | $-0.02** \pm 0.02$   | $0.00 \pm 0.02$   |
| Baseline global $R_1$                   | $0.90 \pm 0.05$        | $0.88* \pm 0.05$     | $0.91 \pm 0.04$   |
| Follow-up global $R_1$                  | $0.90 \pm 0.05$        | $0.88** \pm 0.05$    | $0.92 \pm 0.05$   |
| Annual change global $R_1$              | $-0.00 \pm 0.01$       | $-0.00 \pm 0.02$     | $0.00 \pm 0.01$   |

Amyloid + vs - : \* $p < 0.05$ , \*\* $p < 0.01$ , \*\*\* $p < 0.001$ ; baseline vs follow-up: <sup>a</sup> $p < 0.01$ , <sup>b</sup> $p < 0.001$

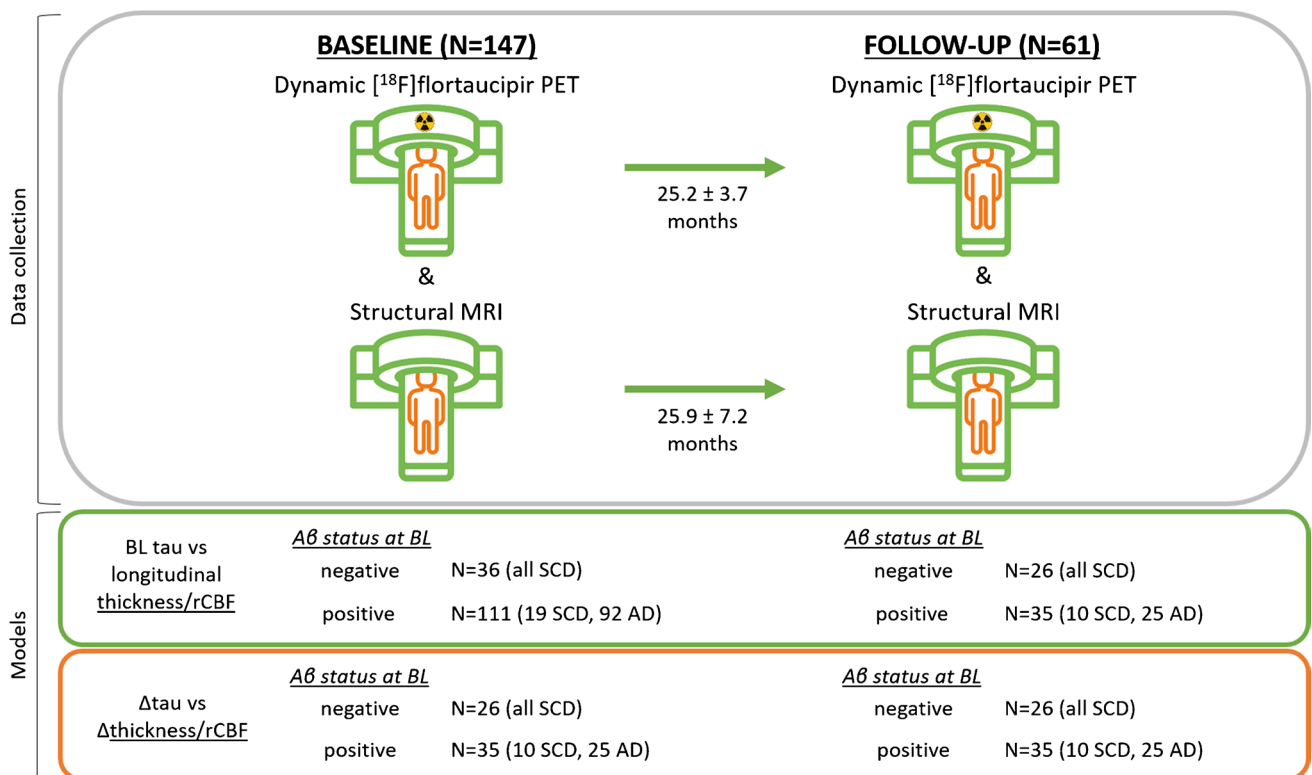


**Fig. 1** Overview of the study design. BL, baseline; rCBF, relative cerebral blood flow; Aβ, amyloid-β; SCD, subjective cognitive decline; AD, symptomatic Alzheimer's disease

canceling each other out when calculating an effect over the whole group; Fig. 2). We therefore did perform the LMMs with longitudinal rCBF as dependent variable.

### Longitudinal cortical thickness as outcome measure

#### Baseline tau PET BP<sub>ND</sub> as determinant

In Aβ+ individuals, linear mixed models showed that higher tau BP<sub>ND</sub> at baseline was associated with cortical thinning over time (Fig. 3). More specifically, tau PET BP<sub>ND</sub> in Braak III/IV was associated with a decrease in cortical thickness over time in widespread cortical regions, including parietal, (medial) frontal, and (lateral) temporal lobes. Comparable results were observed with tau PET BP<sub>ND</sub> in Braak V/VI as the determinant, although with generally lower effect sizes compared to Braak III/IV. Tau PET BP<sub>ND</sub> in Braak I showed only weak associations (not surviving FDR-correction) with cortical thinning over time. In Aβ- individuals, no FDR-surviving associations were found for any of the Braak ROIs (sFigure 1).

#### Annual change tau PET BP<sub>ND</sub> as determinant

Linear mixed models did not yield any FDR-correction surviving associations between annual change in tau PET

BP<sub>ND</sub> and longitudinal cortical thickness in both Aβ+ and Aβ- individuals (sFigure 3).

### Longitudinal rCBF as outcome measure

#### Baseline tau PET BP<sub>ND</sub> as determinant

Linear mixed models yielded no FDR-correction surviving associations between baseline tau PET BP<sub>ND</sub> and longitudinal rCBF in neither Aβ+ nor Aβ- individuals (sFigure 2).

#### Annual change tau PET BP<sub>ND</sub> as determinant

Linear mixed models showed that increases in tau PET BP<sub>ND</sub> over time were associated with increases in R<sub>1</sub> over time in the inferolateral and superior parietal gray matter in Aβ+ individuals (sFigure 4). No associations surviving correction for multiple comparisons were found in Aβ- individuals.

## Discussion

We assessed the associations between tau pathology and neuronal injury (reflected by measures of cortical thickness and rCBF) over time. We showed that higher tau pathology at

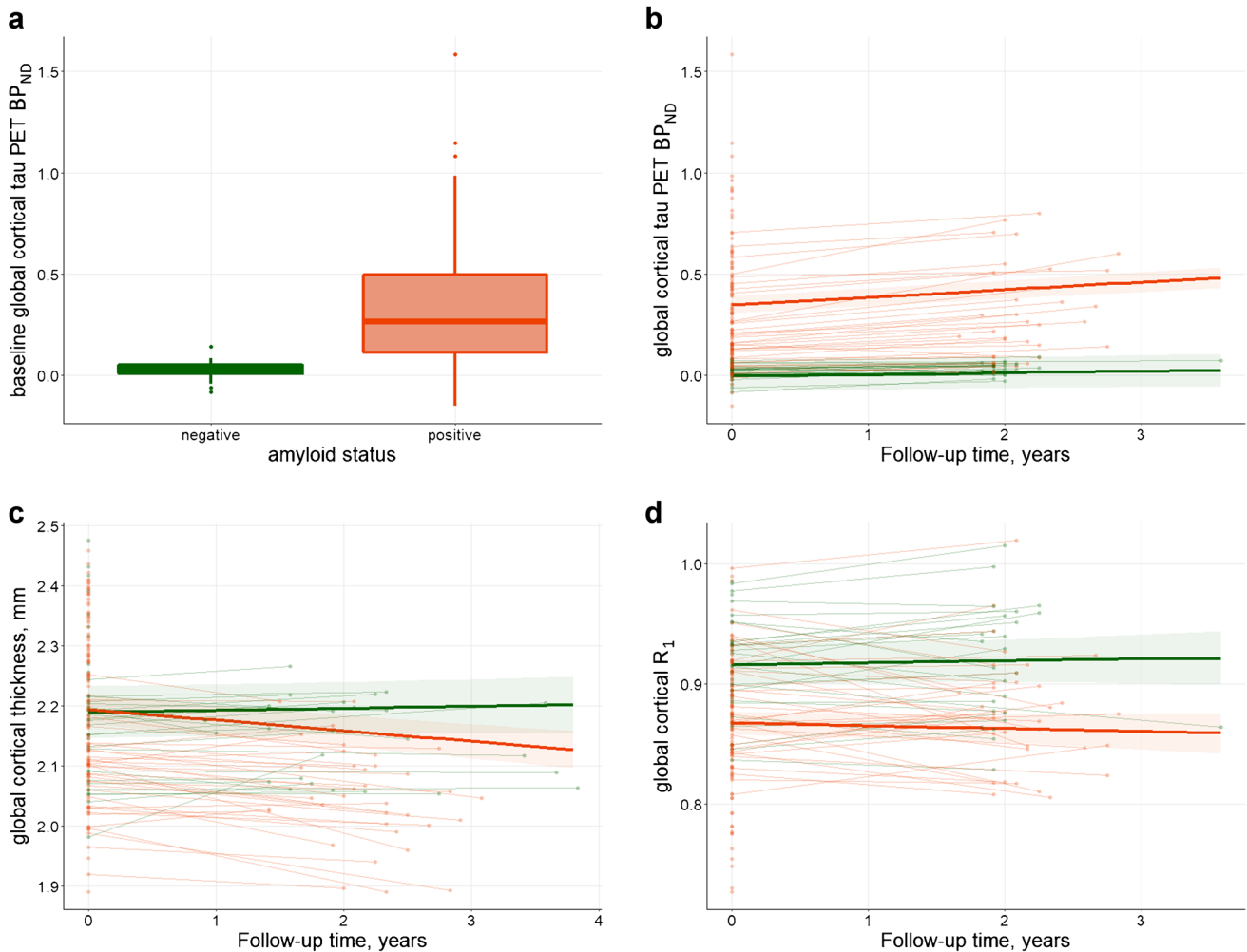


**Fig. 2** Plots showing baseline tau PET  $BP_{ND}$  (a) and longitudinal tau PET  $BP_{ND}$  (b), cortical thickness (c), and  $R_1$  (d) in amyloid negative (green) and positive (red) individuals

baseline (especially in the Braak III/IV region) was associated with faster cortical thinning over time in  $A\beta+$  individuals. Annual change in tau pathology did not show associations with cortical thinning over time, but larger increases in tau pathology did show associations with larger increases in  $R_1$  over time in inferolateral and superior parietal regions in  $A\beta+$  individuals. Our results are in line with disease models proposing that tau load is a key driver of local cortical thinning and stress the need for future longitudinal studies into the role of rCBF in the pathophysiological process of AD. Furthermore, our results indicate that a single tau PET scan at baseline best predicts cortical thinning over time when compared to longitudinal tau PET imaging. This in turn highlights the potential of a single tau PET to improve the prognosis and selection of the right target population for clinical trials.

Our findings of higher tau pathology at baseline predicting cortical thinning over time in  $A\beta+$  individuals are in line with previous studies, demonstrating local and non-local

associations between tau pathology and longitudinal cortical thinning in  $A\beta+$  individuals [2, 5, 11, 12, 40]. Regions most commonly showing associations between tau pathology and cortical thinning over time include frontotemporal and occipitoparietal regions [2, 11, 12, 40], which is similar to our findings, showing the strongest effects for Braak III/IV regional tau pathology and increased cortical thinning in the frontotemporal-parietal regions. We also assessed the association between (annual) change in tau pathology and (annual) change in cortical thickness. Whereas others reported (moderate) associations between larger increases in tau pathology and larger decreases in cortical thickness in individuals with mild cognitive impairment or atypical AD [12, 13], we found no associations surviving correction for multiple testing between change in tau pathology and longitudinal cortical thickness. A potential reason for these differences across studies might be the variance in parameters used. In our study, we used fully quantitative

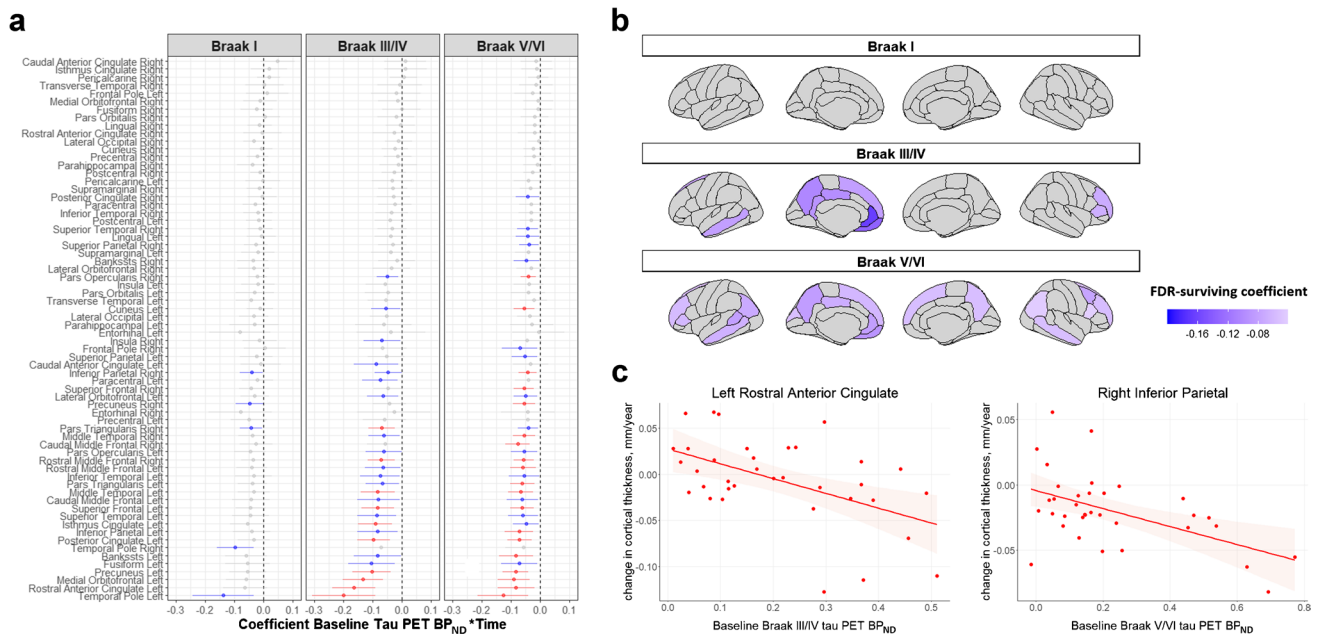


**Fig. 3** Association between baseline tau PET ( $BP_{ND}$ ) and longitudinal cortical thickness (mm) in amyloid-positive individuals. **a** Forest plot showing model estimates with 95% confidence intervals from linear mixed models with baseline tau PET  $BP_{ND}$  as determinant, longitudinal cortical thickness as outcome measure and age,

sex, and time as covariates. Gray = non-significant. Blue =  $p < 0.05$ . Red =  $p_{FDR} < 0.05$ . **b** FDR-surviving results visualized using the ggseg R package. **c** Two scatterplots exemplifying FDR-surviving associations between baseline tau PET  $BP_{ND}$  and longitudinal cortical thickness

tau PET  $BP_{ND}$  to precisely measure (change in) tau pathology, whereas other studies used the semi-quantitative standardized uptake value ratio (SUVr), which is more sensitive to blood flow-introduced bias, specifically in longitudinal settings [41]. However, recently it has been demonstrated that SUVr provides an accurate estimate of specific binding for [ $^{18}F$ ]flortaucipir over a two-year follow-up during which changes in flow are small [42], making this unlikely to be a sole explanation for differences in results between studies. A difference in statistical power might also have played a role, since we did find some associations between larger increases in tau pathology with decreases in cortical thinning in  $A\beta+$  individuals when using a more liberal statistical threshold (without correction for multiple testing). Taken together, in  $A\beta+$  individuals we found robust associations between baseline tau pathology and longitudinal cortical thickness, while no association between change in tau pathology and longitudinal cortical thickness was found. This might be explained by the difference in sample size in the statistical models for baseline tau PET  $BP_{ND}$  ( $n = 147$ ) vs annual change in tau PET  $BP_{ND}$  ( $n = 61$ ) as determinant. It may also be that our follow-up sample was somewhat biased, as the most advanced individuals might have dropped out more frequently. Another reason may be that there is a temporal delay for the neurotoxic effects of tau to manifest, making baseline tau pathology more important for the occurrence of neurodegeneration when compared to change in tau. Lastly,

the magnitude of annual change in tau PET  $BP_{ND}$  is generally modest, leading to a difference in variability which may affect the ability of finding statistically significant effects.

Our results demonstrated an increase in tau pathology over time, irrespective of baseline amyloid status. Although current hypothetical models propose that amyloidosis is an upstream driver of tau accumulation [4, 43, 44], and tau pathology is generally only found to be accumulating in  $A\beta+$  individuals, there are some studies showing significant cortical tau accumulation in  $A\beta-$  individuals [40, 45]. Accumulation of tau pathology in  $A\beta-$  individuals may be driven by processes related to aging, since positive associations between rates of tau accumulation and age were found among cognitively unimpaired  $A\beta-$  individuals [44]. It could also be that  $A\beta-$  individuals with accumulating tau pathology do actually have amyloid pathology, but at subthreshold or below detection levels, as it has previously been shown that in individuals who were nominally  $A\beta-$ , both the rate of  $A\beta$  accumulation and the baseline  $A\beta$  load predicted tau deposition in cortical Braak regions associated with AD [46, 47]. Future studies into longitudinal tau accumulation in the context of amyloid pathology may therefore consider looking at continuous amyloid levels rather than binary amyloid status.

Relative cerebral blood flow did not change over time during the two-year follow-up period. Although longitudinal changes in rCBF have not been studied previously using

[<sup>18</sup>F]flortaucipir  $R_1$  in other cohorts, we might compare our findings with studies investigating CBF using SPECT, <sup>15</sup>O-H<sub>2</sub>O PET, and MRI. Previous findings were indicative of both increases and decreases in rCBF over time in individuals without dementia who had high-amyloid load [24] and decreases in (fast progressing) AD patients [48]. These findings are in contrast with the lack of change over time in our study and also in contrast with our hypothesis, where we assumed that CBF alterations occur in between tau accumulation and atrophy in the pathophysiological development of AD, thus expecting changes in rCBF to occur, especially when changes in cortical thickness are observed. One explanation for this discrepancy might be that changes in rCBF occur in different directions (in- or decreases) on the individual level (as can also be observed in Fig. 2), potentially canceling each other out, leading to absence of average effects or change on the group level. Another explanation may lie in results of another study assessing the relationship between longitudinal perfusion measures and tau pathology (as measured with PET), as they found a lack of overlap between declining perfusion and increases in tau pathology, suggesting a lag phase between these two processes [49]. This may also be the case here, given that tau pathology did change over time, while  $R_1$  did not (yet) in our study. Lastly, an explanation might lie in the composition of our A $\beta$ + group. Some literature describes increases in CBF over time in individuals without dementia with low-, intermediate- or high amyloid load [23, 24]. This might suggest that the increase in CBF represents a compensatory mechanism in response to first-occurring pathology. The fact that our amyloid-positive group also included non-demented individuals, in whom this compensatory increase in CBF potentially takes place, might have contributed to the positive association between increases in Braak III/IV tau pathology and parietal CBF as found in our study.

A strength of the current study is that fully dynamic [<sup>18</sup>F]flortaucipir PET data was used to obtain quantitatively accurate measures of both tau pathology and rCBF in a sample covering the whole AD spectrum (CN-dementia). Furthermore, relative to previous studies this study had a long follow-up period of 25 months. Some caveats are, however, to be considered in the interpretation of our results. First, three different atlases were used to process our data, i.e., Hammers (Braak III–VI) and Svarer (Braak I) for PET and Desikan-Killiany for MRI. We opted not to change our well-established PET pipeline and accept the inherent variations in ROI definitions introduced by this methodological decision. Second, the subset of individuals with longitudinal tau PET data available was relatively small. This may have reduced the statistical power to detect effects. Also, there was likely a bias in our follow-up sample, where older patients and patients with lower MMSE scores dropped out more frequently. This bias is unfortunately common in longitudinal AD studies and

likely excludes more progressed AD patients at follow-up. Furthermore, our sample is relatively young and findings might not translate to older patient populations where co-pathologies (independently of tau pathology) associated with brain atrophy are more common. Last, some of the regions that yielded significant associations, like the temporal poles or orbitofrontal cortices, are known to be susceptible to Free-surfer segmentation errors. However, these regions are found repeatedly throughout the literature and image segmentations were thoroughly checked prior to analyses.

In conclusion, we assessed the association between i) baseline and ii) change in tau pathology with longitudinal atrophy and rCBF by using dynamic [<sup>18</sup>F]flortaucipir PET and structural MRI scans. We demonstrate that tau pathology accumulated in individuals, irrespective of their baseline amyloid status and that cortical thickness decreases over time in A $\beta$ + individuals only. On group level no change in rCBF over the two-year follow-up period was observed, but both in- and decreases were found on the individual level. This stresses the need for future longitudinal studies into complex longitudinal changes in rCBF and their association with (changes in) tau pathology. Furthermore, higher tau pathology at baseline was associated with faster cortical thinning over time in A $\beta$ + individuals. These results support disease models in which tau pathology is a driver of neurodegenerative processes, which will further contribute to potentially establishing the utility of (a single) tau PET as a predictive tool in terms of identifying slow- or fast-degenerating individuals, which may in turn be important for selection criteria in clinical trials.

**Supplementary Information** The online version contains supplementary material available at <https://doi.org/10.1007/s00259-023-06196-2>.

**Acknowledgements** We kindly thank all participants for their contribution. Research of Amsterdam Alzheimer Center is part of the Neurodegeneration program of Amsterdam Neuroscience. The Amsterdam Alzheimer Center is supported by Alzheimer Nederland and Stichting VUmc funds. The chair of Wiesje van der Flier is supported by the Pasmaan stichting. The SCIENCE project receives funding from Gieskes-Strijbis fonds and Stichting Dioraphte. This work was supported by TAP-dementia from ZonMW. [<sup>18</sup>F]Flortaucipir-PET scans were made possible by Avid Radiopharmaceuticals Inc. FB is supported by the NIHR Biomedical Research Centre at UCLH.

**Funding** Research of Alzheimer center Amsterdam has been funded by ZonMW, NWO, EU-FP7, EU-JPND, Alzheimer Nederland, Hersenstichting CardioVascular Onderzoek Nederland, Health-Holland, Topsector Life Sciences & Health, stichting Dioraphte, Gieskes-Strijbis fonds, stichting Equilibrio, Edwin Bouw fonds, Pasmaan stichting, stichting Alzheimer & Neuropsychiatrie Foundation, Philips, Biogen MA Inc, Novartis-NL, Life-MI, AVID, Roche BV, Fujifilm, Combinostics. WF is a recipient of ABOARD, which is a public-private partnership receiving funding from ZonMW (#73305095007) and Health-Holland, Topsector Life Sciences & Health (PPP-allowance; #LSHM20106). The funding sources had no role in the design and conduct of the study; in the collection, analysis, and interpretation of the data; or in the preparation, review, or approval of the manuscript.



**Data Availability** Data can be made available upon reasonable request.

## Declarations

**Conflict of interest** DV, SV, IB, IB, HT, EC, RR, SM, SG, and RO have nothing to disclose.

FB: Steering committee or iDMC member for Biogen, Merck, Roche, Eisai, and Prothena. Consultant for Roche, Biogen, Merck, IXICO, Jansen, and Combinostics. Research agreements with Merck, Biogen, GE Healthcare, and Roche. Co-founder and shareholder of Queen Square Analytics LTD.

WF: Research programs of Wiesje van der Flier have been funded by ZonMW, NWO, EU-FP7, EU-JPND, Alzheimer Nederland, Hersenstichting CardioVascular Onderzoek Nederland, Health~Holland, Topsector Life Sciences & Health, stichting Dioraphte, Gieskes-Strijbis fonds, stichting Equilibrio, Edwin Bouw fonds, Pasman stichting, stichting Alzheimer & Neuropsychiatrie Foundation, Philips, Biogen MA Inc, Novartis-NL, Life-MI, AVID, Roche BV, Fujifilm, Combinostics. WF holds the Pasman chair. WF is a recipient of ABOARD, which is a public-private partnership receiving funding from ZonMW (#73305095007) and Health~Holland, Topsector Life Sciences & Health (PPP-allowance; #LSHM20106). WF has performed contract research for Biogen MA Inc. and Boehringer Ingelheim. WF has been an invited speaker at Boehringer Ingelheim, Biogen MA Inc., Danone, Eisai, WebMD Neurology (Medscape), NovoNordisk, Springer Healthcare, and the European Brain Council. WF is a consultant to Oxford Health Policy Forum CIC, Roche, and Biogen MA Inc. WF participated in advisory boards of Biogen MA Inc, Roche, and Eli Lilly. All funding is paid to her institution. WF is a member of the steering committee of PAVE, and Think Brain Health. WF was associate editor of *Alzheimer, Research & Therapy* in 2020/2021. WF is an associate editor at *Brain*.

**Open Access** This article is licensed under a Creative Commons Attribution 4.0 International License, which permits use, sharing, adaptation, distribution and reproduction in any medium or format, as long as you give appropriate credit to the original author(s) and the source, provide a link to the Creative Commons licence, and indicate if changes were made. The images or other third party material in this article are included in the article's Creative Commons licence, unless indicated otherwise in a credit line to the material. If material is not included in the article's Creative Commons licence and your intended use is not permitted by statutory regulation or exceeds the permitted use, you will need to obtain permission directly from the copyright holder. To view a copy of this licence, visit <http://creativecommons.org/licenses/by/4.0/>.



## References

1. Cho H, Choi JY, Hwang MS, Lee JH, Kim YJ, Lee HM, et al. Tau PET in Alzheimer disease and mild cognitive impairment. *Neurology*. 2016;87:375–83.
2. Gordon BA, McCullough A, Mishra S, Blazey TM, Su Y, Christensen J, et al. Cross-sectional and longitudinal atrophy is preferentially associated with tau rather than amyloid  $\beta$  positron emission tomography pathology. *Alzheimer's Dement Diagn Assess Dis Monit*. 2018;10:245–52.
3. Iaccarino L, Tammewar G, Ayakta N, Baker SL, Bejanin A, Boxer AL, et al. Local and distant relationships between amyloid, tau and neurodegeneration in Alzheimer's Disease. *NeuroImage Clin*. 2018;17:452–64.
4. Jack CR Jr, Knopman DS, Jagust WJ, Petersen RC, Weiner MW, Aisen PS, et al. Tracking pathophysiological processes in Alzheimer's disease: an updated hypothetical model of dynamic biomarkers. *Lancet Neurol*. 2013;12:207–16.
5. La Joie R, Visani AV, Baker SL, Brown JA, Bourakova V, Cha J, et al. Prospective longitudinal atrophy in Alzheimer's disease correlates with the intensity and topography of baseline tau-PET. *Sci Transl Med*. 2020;12:eaa5732.
6. Whitwell J, Josephs K, Murray M, Kantarci K, Przybelski S, Weigand S, et al. MRI correlates of neurofibrillary tangle pathology at autopsy: a voxel-based morphometry study. *Neurology*. 2008;71:743–9.
7. Devous MD, Joshi AD, Navitsky M, Southeikal S, Pontecorvo MJ, Shen H, et al. Test-retest reproducibility for the tau PET imaging agent Flortaucipir F 18. *J Nucl Med*. 2018;59:937–43.
8. Schöll M, Maass A, Mattsson N, Ashton NJ, Blennow K, Zetterberg H, et al. Biomarkers for tau pathology. *Mol Cell Neurosci*. 2019;97:18–33.
9. Timmers T, Ossenkoppele R, Visser D, Tuncel H, Wolters EE, Verfaillie SC, et al. Test-retest repeatability of [18F] Flortaucipir PET in Alzheimer's disease and cognitively normal individuals. *J Cereb Blood Flow Metab*. 2020;40:2464–74.
10. Timmers T, Ossenkoppele R, Wolters EE, Verfaillie SC, Visser D, Golla SS, et al. Associations between quantitative [18F] flortaucipir tau PET and atrophy across the Alzheimer's disease spectrum. *Alzheimer's Res Ther*. 2019;11:1–12.
11. Das SR, Xie L, Wisse LE, Ittyerah R, Tustison NJ, Dickerson BC, et al. Longitudinal and cross-sectional structural magnetic resonance imaging correlates of AV-1451 uptake. *Neurobiol Aging*. 2018;66:49–58.
12. Sintini I, Martin PR, Graff-Radford J, Senjem ML, Schwarz CG, Machulda MM, et al. Longitudinal tau-PET uptake and atrophy in atypical Alzheimer's disease. *NeuroImage Clin*. 2019;23:101823.
13. Xu G, Zheng S, Zhu Z, Yu X, Jiang J, Jiang J, et al. Association of tau accumulation and atrophy in mild cognitive impairment: a longitudinal study. *Ann Nucl Med*. 2020;34:815–23.
14. Visser D, Wolters EE, Verfaillie SC, Coomans EM, Timmers T, Tuncel H, et al. Tau pathology and relative cerebral blood flow are independently associated with cognition in Alzheimer's disease. *Eur J Nucl Med Mol Imaging*. 2020;47:3165–75.
15. Heeman F, Visser D, Yaqub M, Verfaillie S, Timmers T, Pijnenburg YA, et al. Precision estimates of relative and absolute cerebral blood flow in Alzheimer's disease and cognitively normal individuals. *J Cereb Blood Flow Metab*. 2022;0271678X221135270.
16. Ottoy J, Verhaeghe J, Niemantsverdriet E, De Roeck E, Ceysens S, Van Broeckhoven C, et al. 18F-AV45 PET, the early phases and the delivery rate of 18F-AV45 PET as proxies of cerebral blood flow in Alzheimer's disease: Validation against 15O-H<sub>2</sub>O PET. *Alzheimer's Dementia*. 2019;15:1172–82.
17. Peretti DE, Vázquez García D, Reesink FE, Doorduyn J, de Jong BM, De Deyn PP, et al. Diagnostic performance of regional cerebral blood flow images derived from dynamic PIB scans in Alzheimer's disease. *EJNMMI Res*. 2019;9:1–9.
18. Peretti DE, Vázquez García D, Reesink FE, van der Goot T, De Deyn PP, de Jong BM, et al. Relative cerebral flow from dynamic PIB scans as an alternative for FDG scans in Alzheimer's disease PET studies. *PLoS ONE*. 2019;14: e0211000.
19. Korte N, Nortley R, Attwell D. Cerebral blood flow decrease as an early pathological mechanism in Alzheimer's disease. *Acta Neuropathol*. 2020;140:793–810.
20. Sweeney MD, Kisler K, Montagne A, Toga AW, Zlokovic BV. The role of brain vasculature in neurodegenerative disorders. *Nat Neurosci*. 2018;21:1318–31.
21. Ahmadi K, Pereira JB, Berron D, Vogel J, Ingala S, Strandberg OT, et al. Gray matter hypoperfusion is a late pathological event in the course of Alzheimer's disease. *J Cereb Blood Flow Metab*. 2022;43(4):565–580. <https://doi.org/10.1177/0271678X221141139>.

22. Jack CR Jr, Bennett DA, Blennow K, Carrillo MC, Dunn B, Haeberlein SB, et al. NIA-AA research framework: toward a biological definition of Alzheimer's disease. *Alzheimer's Dement.* 2018;14:535–62.
23. Ebenau JL, Visser D, Verfaillie SC, Timmers T, van Leeuwenstijn MS, Kate MT, et al. Cerebral blood flow, amyloid burden, and cognition in cognitively normal individuals. *Eur J Nucl Med Mol Imaging.* 2023;50(2):410–422.
24. Sojkova J, Beason-Held L, Zhou Y, An Y, Kraut MA, Ye W, et al. Longitudinal cerebral blood flow and amyloid deposition: an emerging pattern? *J Nucl Med.* 2008;49:1465–71.
25. Van Der Flier WM, Scheltens P. Amsterdam dementia cohort: performing research to optimize care. *J Alzheimer's Dis.* 2018;62:1091–111.
26. Jessen F, Amariglio RE, Van Boxtel M, Breteler M, Ceccaldi M, Chételat G, et al. A conceptual framework for research on subjective cognitive decline in preclinical Alzheimer's disease. *Alzheimer's Dement.* 2014;10:844–52.
27. Albert MS, DeKosky ST, Dickson D, Dubois B, Feldman HH, Fox NC, et al. The diagnosis of mild cognitive impairment due to Alzheimer's disease: recommendations from the National Institute on Aging-Alzheimer's Association workgroups on diagnostic guidelines for Alzheimer's disease. *Focus.* 2013;11:96–106.
28. McKhann GM, Knopman DS, Chertkow H, Hyman BT, Jack CR Jr, Kawas CH, et al. The diagnosis of dementia due to Alzheimer's disease: recommendations from the National Institute on Aging-Alzheimer's Association workgroups on diagnostic guidelines for Alzheimer's disease. *Alzheimer's Dement.* 2011;7:263–9.
29. Slot RE, Verfaillie SC, Overbeek JM, Timmers T, Wesselman LM, Teunissen CE, et al. Subjective Cognitive Impairment Cohort (SCIENCE): study design and first results. *Alzheimer's Res Ther.* 2018;10:1–13.
30. Tijms BM, Willems EA, Zwan MD, Mulder SD, Visser PJ, van Berckel BN, et al. Unbiased approach to counteract upward drift in cerebrospinal fluid amyloid- $\beta$  1–42 analysis results. *Clin Chem.* 2018;64:576–85.
31. Golla SS, Timmers T, Ossenkoppele R, Groot C, Verfaillie S, Scheltens P, et al. Quantification of tau load using [18F] AV1451 PET. *Mol Imag Biol.* 2017;19:963–71.
32. Tuncel H, Visser D, Yaqub M, Timmers T, Wolters EE, Ossenkoppele R, et al. Effect of Shortening the Scan Duration on Quantitative Accuracy of [18F] Flortaucipir Studies. *Mol Imag Biol.* 2021;23:604–13.
33. Hammers A, Allom R, Koeppe MJ, Free SL, Myers R, Lemieux L, et al. Three-dimensional maximum probability atlas of the human brain, with particular reference to the temporal lobe. *Hum Brain Mapp.* 2003;19:224–47.
34. Svarer C, Madsen K, Hasselbalch SG, Pinborg LH, Haugbøl S, Frøkjær VG, et al. MR-based automatic delineation of volumes of interest in human brain PET images using probability maps. *Neuroimage.* 2005;24:969–79.
35. Gunn RN, Lammertsma AA, Hume SP, Cunningham VJ. Parametric imaging of ligand-receptor binding in PET using a simplified reference region model. *Neuroimage.* 1997;6:279–87.
36. Golla SS, Wolters EE, Timmers T, Ossenkoppele R, van der Weijden CW, Scheltens P, et al. Parametric methods for [18F] flortaucipir PET. *J Cereb Blood Flow Metab.* 2020;40:365–73.
37. Reuter M, Schmansky NJ, Rosas HD, Fischl B. Within-subject template estimation for unbiased longitudinal image analysis. *Neuroimage.* 2012;61:1402–18.
38. Desikan RS, Ségonne F, Fischl B, Quinn BT, Dickerson BC, Blacker D, et al. An automated labeling system for subdividing the human cerebral cortex on MRI scans into gyral based regions of interest. *Neuroimage.* 2006;31:968–80.
39. Lindroth H, Nair VA, Stanfield C, Casey C, Mohanty R, Wayer D, et al. Examining the identification of age-related atrophy between T1 and T1+ T2-FLAIR cortical thickness measurements. *Sci Rep.* 2019;9:1–11.
40. Harrison TM, La Joie R, Maass A, Baker SL, Swinnerton K, Fenton L, et al. Longitudinal tau accumulation and atrophy in aging and Alzheimer disease. *Ann Neurol.* 2019;85:229–40.
41. van Berckel BN, Ossenkoppele R, Tolboom N, Yaqub M, Foster Dingley JC, Windhorst AD, et al. Longitudinal amyloid imaging using 11C-PiB: methodologic considerations. *J Nucl Med.* 2013;54:1570–6.
42. Visser D, Tuncel H, Ossenkoppele R, Yaqub MM, Wolters EE, Timmers T, et al. Longitudinal tau PET using 18F-flortaucipir: the Effect of relative Cerebral Blood Flow on (semi) quantitative parameters. *J Nucl Med.* 2022;64(2):281–286.
43. Pontecorvo MJ, Devous MD Sr, Navitsky M, Lu M, Salloway S, Schaerf FW, et al. Relationships between flortaucipir PET tau binding and amyloid burden, clinical diagnosis, age and cognition. *Brain.* 2017;140:748–63.
44. Jack CR Jr, Wiste HJ, Schwarz CG, Lowe VJ, Senjem ML, Vemuri P, et al. Longitudinal tau PET in ageing and Alzheimer's disease. *Brain.* 2018;141:1517–28.
45. Leuzy A, Smith R, Cullen NC, Strandberg O, Vogel JW, Binette AP, et al. Biomarker-based prediction of longitudinal tau positron emission tomography in Alzheimer disease. *JAMA Neurol.* 2022;79:149–58.
46. Leal SL, Lockhart SN, Maass A, Bell RK, Jagust WJ. Sub-threshold amyloid predicts tau deposition in aging. *J Neurosci.* 2018;38:4482–9.
47. Reimand J, Collij L, Scheltens P, Bouwman F, Ossenkoppele R, Initiative AsDN. Association of amyloid- $\beta$  CSF/PET discordance and tau load 5 years later. *Neurology.* 2020;95:e2648–e57.
48. Hanyu H, Sato T, Hirao K, Kanetaka H, Iwamoto T, Koizumi K. The progression of cognitive deterioration and regional cerebral blood flow patterns in Alzheimer's disease: a longitudinal SPECT study. *J Neurol Sci.* 2010;290:96–101.
49. Leuzy A, Rodriguez-Vieitez E, Saint-Aubert L, Chiotis K, Almkvist O, Savitcheva I, et al. Longitudinal uncoupling of cerebral perfusion, glucose metabolism, and tau deposition in Alzheimer's disease. *Alzheimer's Dement.* 2018;14:652–63.

**Publisher's note** Springer Nature remains neutral with regard to jurisdictional claims in published maps and institutional affiliations.

## Authors and Affiliations

Denise Visser<sup>1,2,3</sup>  · Sander C. J. Verfaillie<sup>1,2,3,4</sup> · Iris Bosch<sup>1,3,5,6</sup> · Iman Brouwer<sup>1,2,3</sup> · Hayel Tuncel<sup>1,2,3</sup> · Emma M. Coomans<sup>1,2,3</sup> · Roos M. Rikken<sup>1,2,3</sup> · Sophie E. Mastenbroek<sup>1,2,3,7</sup> · Sandeep S. V. Golla<sup>1,2,3</sup> · Frederik Barkhof<sup>1,2,3,8</sup> · Elsmarieke van de Giessen<sup>1,2,3</sup> · Bart N. M. van Berckel<sup>1,2,3</sup> · Wiesje M. van der Flier<sup>2,9,10</sup> · Rik Ossenkoppele<sup>2,7,9</sup> 

<sup>1</sup> Department of Radiology & Nuclear Medicine, Amsterdam Neuroscience, Vrije Universiteit Amsterdam, Amsterdam UMC, P.O. Box 7057, 1007 MB Amsterdam, The Netherlands

<sup>2</sup> Amsterdam Neuroscience, Neurodegeneration, Amsterdam, The Netherlands

<sup>3</sup> Amsterdam Neuroscience, Brain Imaging, Amsterdam, The Netherlands

<sup>4</sup> Medical Psychology, Amsterdam UMC Location University of Amsterdam, Meibergdreef 9, Amsterdam, the Netherlands

<sup>5</sup> Department of Psychiatry and Neurochemistry, Institute of Neuroscience and Physiology, The Sahlgrenska Academy, University of Gothenburg, Gothenburg, Sweden

<sup>6</sup> Wallenberg Centre for Molecular and Translational Medicine, University of Gothenburg, Gothenburg, Sweden

<sup>7</sup> Clinical Memory Research Unit, Lund University, Lund, Sweden

<sup>8</sup> Institutes of Neurology and Healthcare Engineering, University College London, London, UK

<sup>9</sup> Alzheimer Center Amsterdam, Department of Neurology, Amsterdam Neuroscience, Vrije Universiteit Amsterdam, Amsterdam UMC location VUmc, Amsterdam, The Netherlands

<sup>10</sup> Department of Epidemiology and Data Science, Vrije Universiteit Amsterdam, Amsterdam UMC, Amsterdam, The Netherlands